

OPEN

Observer variability in the assessment of renal ^{18}F -FDG uptake in kidney transplant recipients

Alexandre Jadoul^{1,5}, Pierre Lovinfosse^{1,5}, Antoine Bouquegneau², Laurent Weekers², Hans Pottel³, Roland Hustinx¹ & François Jouret^{2,4*}

^{18}F -FDG PET/CT imaging may help non-invasively disprove the diagnosis of acute kidney allograft rejection (AR) in kidney transplant recipients (KTR). The present study aims at evaluating the repeatability and reproducibility of the quantification of renal ^{18}F -FDG uptake in KTR. We prospectively performed ^{18}F -FDG PET/CT in 95 adult KTR who underwent surveillance transplant biopsy between 3 to 6 months *post* transplantation. Images were obtained 180 minutes after injecting 3 MBq ^{18}F -FDG per kg body weight. Mean standard uptake value (SUV_{mean}) of kidney cortex was independently measured by 2 experienced observers in 4 volumes of interest (VOI) distributed in the upper ($n = 2$) and lower ($n = 2$) poles. The first observer repeated SUV assessment in the uppermost VOI, blinded to the initial results. Intra-class correlation coefficients (ICC) and Bland-Altman plots were calculated. An ICC of 0.96 with 95%CI of [0.94; 0.97] was calculated for the intra-observer measurements. The ICC for inter-observer reproducibility for each VOI was 0.87 [0.81–0.91], 0.87 [0.81–0.91], 0.85 [0.78–0.89] and 0.83 [0.76–0.88] for the upper to the lower renal poles, respectively. The repeatability and reproducibility of the quantification of kidney allograft ^{18}F -FDG uptake are both consistent, which makes it transferrable to the clinical routine.

Kidney transplantation represents the treatment of choice for patients with end stage renal disease¹. Despite the steady progress of immunosuppressive treatments, acute rejection (AR) remains a recurrent complication which impacts both graft and patient survivals^{2,3}. Furthermore, systematic studies focusing on the clinical value of protocol biopsies (by definition performed in stable kidney transplant recipients (KTR)) have demonstrated a non-negligible prevalence of subclinical AR^{4–8}. By definition, subclinical AR corresponds to “the histological documentation of unexpected evidence of AR in a stable patient”⁹. Early management of AR decreases the risk of chronic cellular/humoral rejection, late AR episodes and improves long-term graft survival in KTR¹⁰. Therefore, precocious detection of (subclinical) AR is essential.

In current clinical practice, transplant needle biopsy (TNB) using Banff classification is the gold standard for AR diagnosis¹¹. Still, it is associated with a substantial risk of complications, such as hemorrhage or infection¹². Thus, non-invasive approaches have been developed over the past decades in order to help clinicians avoid potential side effects of TNB^{13–15}. Particularly, promising preclinical and clinical observations have been reported on the role of ^{18}F -fluorodeoxyglucose (^{18}F -FDG) positron-emission tomography coupled with computed tomography (PET/CT) in kidney allograft AR, in both diagnosis and therapeutic monitoring^{16–18}. One may speculate that the AR-induced recruitment of activated leukocytes – with high metabolic activity – increases the uptake of ^{18}F -FDG in renal graft cortex¹⁹.

In addition to the visual assessment, PET/CT allows a semi-quantitative analysis of the images which is reflected by standardized uptake value (SUV). SUV represents the decay-corrected concentration of intravenously injected ^{18}F -FDG in a volume of interest (VOI). Doing so, we demonstrated a significant link between cortical renal graft SUV_{mean} and Banff score, with sensitivity and specificity in diagnosing AR of 100% and 50%, respectively, using a threshold of 1.6¹⁶. However, many well-known factors may affect the accuracy of SUV measurement, including patient weight, blood glucose level, time between the injection of the ^{18}F -FDG and image

¹Division of Nuclear Medicine and oncological imaging, University Hospital of Liege, Liege, Belgium. ²Division of Nephrology, Department of Internal Medicine, University Hospital of Liege, Liege, Belgium. ³Department of Public Health and Primary Care, KU Leuven Campus Kulak Kortrijk, Kortrijk, Belgium. ⁴Groupe Interdisciplinaire de Génomique Appliquée, Cardiovascular Sciences, University of Liège, Liège, Belgium. ⁵These authors contributed equally: Alexandre Jadoul and Pierre Lovinfosse. *email: francois.jouret@chuliege.be

acquisition, partial-volume effect, and recovery coefficient. Additionally, VOI delineation, which is the sole parameter dependent on the physician, may bias the quantification of renal ^{18}F -FDG uptake²⁰. The segmentation of kidney transplant is especially important in order to avoid VOI contamination by the physiological activity linked to the urine excretion of the radiotracer. The purpose of this study is therefore to evaluate the intra- and inter-observer variability in the assessment of renal ^{18}F -FDG uptake in KTR.

Material and Methods

Patients. From November 2015 to January 2018, we prospectively performed an ^{18}F -FDG PET/CT imaging in KTR undergoing a surveillance transplant biopsy between 3 to 6 months post transplantation. Patients with delayed protocol biopsy (>6 months), under 18 years, who underwent transplantectomy, or who were pregnant or breastfeeding were all excluded. Estimated glomerular filtration rate (eGFR) was calculated using modification of diet in renal disease (MDRD) equation. The study was approved by the institutional review board of the University of Liege.

^{18}F -FDG PET/CT. PET/CT was performed using cross-calibrated Philips GEMINI TF Big Bore or TF 16 PET/CT systems (Philips Medical Systems, Cleveland, OH). Low-dose helical CT (5-mm slice thickness, 120-kV tube voltage, and 40-mAs tube current-time product) was followed by a PET emission scanning with 2 bed positions each lasting 240 seconds. Image reconstruction involved iterative list mode time-of-flight algorithms. Corrections for attenuation, dead time, random, and scatter events were applied.

Mean standard uptake value (SUV_{mean}) of kidney cortex was measured by 2 observers (board-certified physicians in nuclear medicine with 9 and 5 year-experience in ^{18}F -FDG PET/CT imaging) in 4 VOI of 1 mL distributed in the upper ($n = 2$) and lower ($n = 2$) poles at distance of the pelviclyceal zone. There was no *a priori* minimal threshold of distance to draw the VOI from the urinary pelvis. One VOI of 20 mL was drawn in the psoas muscle. The observer 1 repeated SUV assessment in the uppermost VOI, blinded to the initial results. SUV_{mean} of each VOI was calculated with the following formula: $[\text{Voxel Value (Bq/mL)} \times \text{Patient Weight (kg)}] / [\text{Injected Dose (Bq)} \times 1000 \text{ (g/kg)}]$. On average, it takes ~5 minutes to measure the SUV_{mean} of the renal cortex and the psoas muscle per patient.

Statistics. To measure the agreement between the results (intra- and inter-observer variability), the following statistical methods were used: Repeated measures ANOVA, Bland and Altman's graph, and intra-class correlation coefficient (ICC). ICC is a measure of the agreement between two methods when the studied variable is continuous. Closer the ICC is to 1, better is the agreement between the two measurements. The results are considered significant at the significance level of 5% ($p < 0.05$).

Ethical approval and consent to participate. All procedures were performed in accordance with the principles of the 1964 Declaration of Helsinki and its later amendments or comparable ethical standards. The study design and exemption from informed consent were approved by the Institutional Review Board of Liege University Hospital.

Results

Ninety-five adult KTR underwent one PET/CT between November 2015 and January 2018, within 3 to 6 months following the transplantation. The mean age of the cohort was 54 ± 13 years (Range: 19–73 y.), with a male to female ratio of 2.4. Characteristics of the cohort are summarized in Table 1. PET/CT was performed in fasting conditions 195 ± 14 (Range: 174–231) min after injection of 245 ± 32 (Range: 156–350) MBq of ^{18}F -FDG. Mean glycemia was 109 ± 27 (Range: 62–241) mg/dL.

The values of kidney transplant SUV_{mean} were, from top to bottom, 1.51 ± 0.40 (Range: 0.54–2.73), 1.54 ± 0.36 (Range: 0.6–2.44), 1.55 ± 0.36 (Range: 0.65–2.57), 1.56 ± 0.37 (Range: 0.64–2.68) in observer 1 and 1.53 ± 0.37 (Range: 0.51–2.53), 1.55 ± 0.38 (Range: 0.57–2.44), 1.58 ± 0.39 (Range: 0.65–2.53), 1.58 ± 0.38 (Range: 0.56–2.5) in observer 2. No significant difference was observed between the SUV_{mean} of the 4 VOIs of the same kidney ($p = 0.41$) in observer 1, while SUV_{mean} of the superior pole was significantly lower than the 3 others values in observer 2 ($p = 0.0001$). There was a strong correlation between the 2 observers with ICC values of 0.87, 0.87, 0.85 and 0.83, respectively for each VOI. A slightly better correlation was observed when considering the mean of the 4 values (ICC: 0.90) (Fig. 1), but with no significant difference compared to correlation for each pole (p -value = 0.29, 0.26, 0.11, 0.06). Bland Altman analyses showed mean differences of -0.01 [-0.07 ; $+0.04$], -0.01 [-0.06 ; $+0.04$] for the upper poles and -0.03 [-0.08 ; $+0.03$], -0.02 [-0.08 ; $+0.04$] for the lower poles. The difference for the mean of these values was -0.02 [-0.06 ; $+0.03$] (Fig. 2). Concerning the repeatability, the agreement was calculated for the intra-observer measurements (ICC: 0.96) (Fig. 3), with mean difference of -0.04 [-0.07 ; -0.01] in Bland Altman graph (Fig. 4). The same statistics were performed for SUV_{max} and showed lower values both for ICC and Bland Altman analyses (Annex 1).

Finally, no significant relationship was highlighted between MDRD-based stages of chronic kidney disease (CKD) and the value of the ratio between mean kidney SUV_{mean} and SUV_{mean} of the psoas muscle ($p = 0.24$) (Fig. 5).

Discussion

^{18}F -FDG PET/CT functional imaging is a promising tool in the assessment of AR-associated inflammation^{16,21,22}. This rapid imaging technique does not cause any side-effect in patients with renal failure from normal to mildly reduced GFR to end-stage renal disease. Furthermore, we have recently showed that ^{18}F -FDG PET/CT may help rule out subclinical rejection in stable KTR, with a negative predictive value of 98%²³. Our results support conclusions of previous studies which showed that the uptake of ^{18}F -FDG by kidneys in non-transplant patients and in KTR is not influenced by renal function^{24,25}, and that the alteration of GFR does not significantly compromise

		Cohort (n = 95)
Recipients	Sex [M/F (n); sex ratio]	67/28; 2.4
	BMI (Kg/m ²) mean ± stand dev	26 ± 4
	PRA max (n) [<5%/5%–85%/>85%]	86/6/3
Donors	Sex [M/F (n); sex ratio]	57/38; 1.5
	Donor type (n) [DBD/DCD/LD]	69/20/6
	BMI (Kg/m ²) mean ± stand dev	25 ± 5
Transplantation	Rank (n)[1st/2nd/3rd]	84/9/2
	CIT (min) mean ± stand dev	699 ± 289
	HLA mm mean ± stand dev	
	A	0.89 ± 0.69
	B	1.21 ± 0.64
	DR	0.73 ± 0.57
Status at the time of biopsy	Early graft function (n) [immediate/slow/delayed]	67/19/9
	Maintenance immunosuppression (n)	
	-CNI [CsA/FK/none]	
	-Antimetabolite	2/93/0
	[MMF/MPA/AZA/none]	
	-mTOR inhibitor [yes/no]	82/7/0/6
	-Steroids [yes/no]	1/94
		93/2
	Number of days between KTx and biopsy (mean ± SD)	105 ± 27
Creatinine (mg/dL) mean ±SD	1.41 ± 0.44	
Type of rejection	None/Borderline/Cellular Rejection	73/16/6

Table 1. Characteristics of the population. Abbreviations: AZA, azathioprine; BMI, body mass index; CNI, calcineurin inhibitors; CS, Corticosteroids; CsA, cyclosporin A; DCD, donor after circulatory death; DBD, donor after brain death; FK, tacrolimus; KTx, kidney transplantation; LD, living donor; MMF, mycophenolate mofetyl; MPA, mycophenolic acid; mTOR, mammalian target of rapamycin.

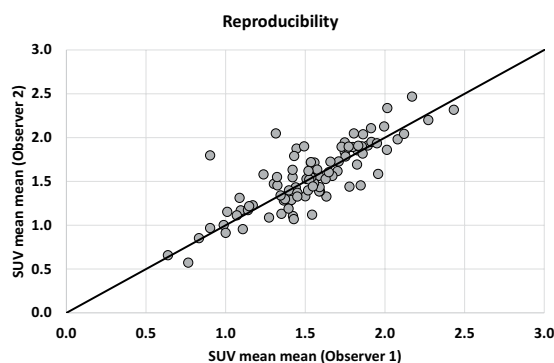


Figure 1. Correlation of mean of SUV_{mean} of the 4 VOI between observer 1 and observer 2. The line depicts the perfect concordance.

the clearance of background activity²⁶. Moreover, the physiological urinary excretion of ¹⁸F-FDG may hamper the measurement of ¹⁸F-FDG uptake in the renal parenchyma²⁷. To overcome this problem, we performed late acquisitions and drew multiple VOI. Although the SUV_{max} has shown the lower inter-observer variability in tumors^{28,29}, we elected to use the SUV_{mean} in order to limit the impact of a potential urinary contamination in the VOI. Doing so, we observed a consistent agreement between the two observers for all VOI. The agreement was the best in the upper pole (ICC: 0.87). No previous data are available in the literature since ¹⁸F-FDG PET/CT imaging has been very recently tested in AR diagnosis in KTR¹⁶. However, Huang *et al.*²⁹ and Büyükdere *et al.*³⁰ have demonstrated a high inter-observer correlation of SUV_{mean} in the evaluation of 43 pulmonary nodules (ICC: 0.97) and 97 lung lesions (ICC: 0.98), respectively. Benz *et al.*²⁸ and Goh *et al.*³¹ also proved a strong reproducibility of SUV_{mean} assessment in treatment monitoring by ¹⁸F-FDG PET/CT in 33 patients with sarcoma (CCC: 0.84) and in the characterization of colorectal tumors (ICC: 0.85). The analysis of intra-observer variability has shown similar results with a high correlation between repeated measurements by the same physician^{30,31}.

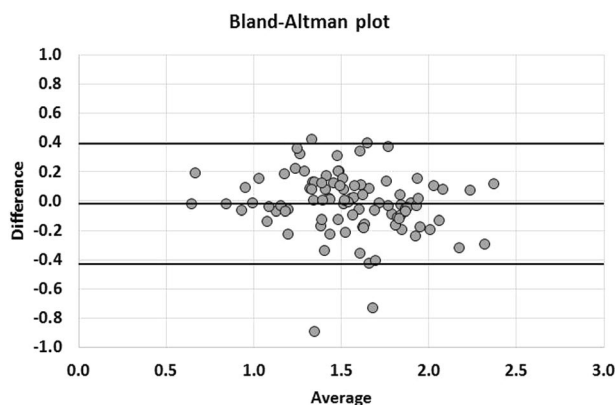


Figure 2. Bland-Altman graph of mean of SUV_{mean} of the 4 VOI. The middle line represents the average of the differences between observer 1 and observer 2 and the two other lines the mean of the differences ± 1.96 standard deviations.

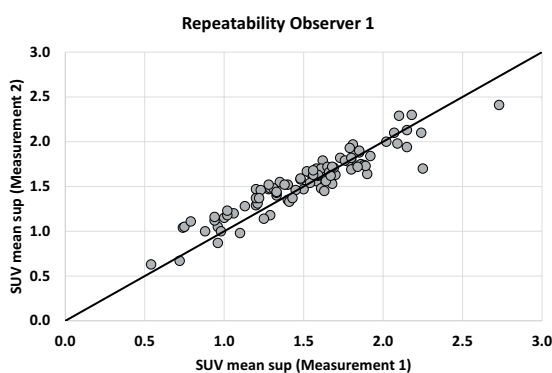


Figure 3. Correlation of SUV_{mean} of the uppermost VOI between measurement 1 and measurement 2 by the same physician. The line depicts the perfect concordance.

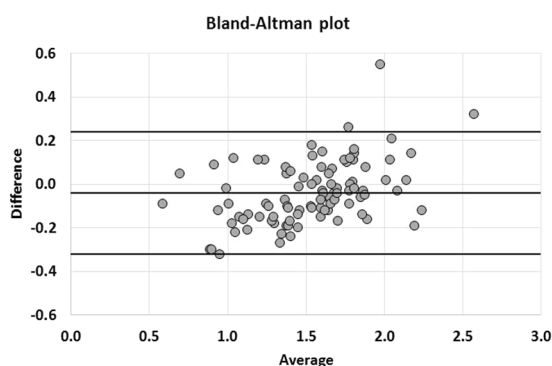


Figure 4. Bland-Altman graph of SUV_{mean} of the uppermost VOI. The middle line represents the average of the differences between measurement 1 and measurement 2 by the same physician and the two other lines the mean of the differences ± 1.96 standard deviations.

Despite the absence of significant difference between ICC of the mean of SUV_{mean} and SUV_{mean} of each pole, superior pole SUV_{mean} of observer 2 was significantly lower than the 3 other values. Furthermore, even if the delineation of only one single VOI is easier in clinical routine, we must keep in mind that histopathological changes in the kidney allograft may not be homogeneous. Sorof *et al.*³² highlighted discordances in histological grading in 30% and therapeutic defects in 7.5% of cases with only one analyzed sample. Automatic kidney component segmentation methods are currently under development and validation. Such an approach may help improve PET/CT-based diagnosis of kidney allograft rejection³³. As a whole, we currently recommend to draw multiple VOI within the renal parenchyma rather than only one.

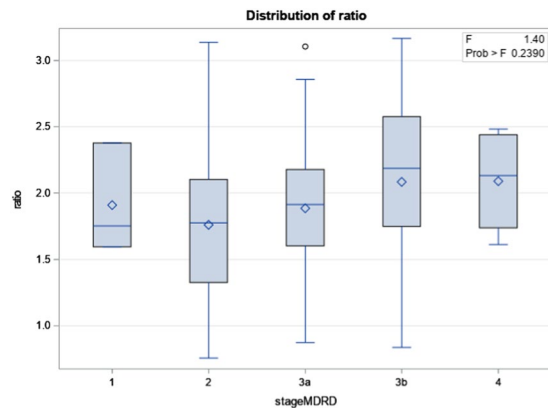


Figure 5. Correlation between estimated eGFR calculated by MDRD equation and ratio of mean kidney $SUV_{\text{mean}}/SUV_{\text{mean}}$ psoas. (n stage 1 = 3, n stage 2 = 25, n stage 3a = 35, n stage 3b = 28, n stage 4 = 4).

Although simplicity and ease of use are among the strengths of SUV, the measurement is nevertheless vulnerable to many sources of unwanted variability²⁰. Despite a careful attention to protocol during the acquisition, there is still a within-subject coefficient of variation in SUV_{mean} reaching 10% for tumours (4.8 to 17.7 depending of the studies)³⁴ and 10–15% for normal tissues³⁵. This variability could be problematic for “borderline” cases with SUV right next to cutoff values.

Conclusions

This study shows that assessment of renal ^{18}F -FDG uptake in KTR is highly repeatable and reproducible if ^{18}F -FDG PET/CT images are evaluated by experienced observers with careful attention to the technique.

Data availability

The datasets used and/or analysed during the current study are available from the corresponding author on reasonable request.

Received: 8 December 2019; Accepted: 12 February 2020;

Published online: 12 March 2020

References

- Wolfe, R. A. *et al.* Comparison of mortality in all patients on dialysis, patients on dialysis awaiting transplantation, and recipients of a first cadaveric transplant. *N. Engl. J. Med.* **341**, 1725–1730 (1999).
- Koo, E. H. *et al.* The impact of early and late acute rejection on graft survival in renal transplantation. *Kidney Res Clin Pract. Sep*; **34**(3):160–4 (2015).
- Jalalzadeh, M., Mousavinasab, N., Peyrovi, S. & Ghadiani, M. H. The impact of acute rejection in kidney transplantation on long-term allograft and patient outcome. *Nephrourol Mon.*, **7** (2015).
- Rush, D. N., Jeffery, J. R. & Gough, J. Sequential protocol biopsies in renal transplant patients. Clinico-pathological correlations using the Banff schema. *Transplant.* **59**, 511 (1995).
- Nankivell, B. J. *et al.* Effect of histological damage on long-term kidney transplant outcome. *Transplant.* **71**, 515 (2001).
- Veronese, F. V. *et al.* Protocol biopsies in renal transplant patients: three-years’ follow-up. *Transpl. Proc.* **34**, 500 (2002).
- Moreso, F. *et al.* Subclinical rejection associated with chronic allograft nephropathy in protocol biopsies as a risk factor for late graft loss. *Am. J. Transplant.* **6**, 747–752 (2006).
- Anil Kumar, M. S. *et al.* Long-term outcome of early steroid withdrawal after kidney transplantation in African American recipients monitored by surveillance biopsy. *Am. J. Transplant.* **8**, 574–585 (2008).
- Racusen, L. C. *et al.* The Banff 97 working classification of renal allograft pathology. *Kidney Int. Feb*; **55**(2), 713–23 (1999).
- Rush, D. *et al.* Beneficial effects of treatment of early subclinical rejection: a randomized study. *J Am Soc Nephrol. Nov*; **9**(11), 2129–34 (1998).
- Haas, M. *et al.* The Banff 2017 Kidney Meeting Report: Revised diagnostic criteria for chronic active T cell-mediated rejection, antibody-mediated rejection, and prospects for integrative endpoints for next-generation clinical trials. *Am J Transplant.* Feb; **18**(2), 293–307 (2018).
- Morgan, T. A., Chandran, S., Burger, I. M., Zhang, C. A. & Goldstein, R. B. Complications of Ultrasound-Guided Renal Transplant Biopsies. *Am J Transplant.* Apr; **16**(4), 1298–305 (2016).
- Thölkling, G., Schuette-Nuetgen, K., Kentrup, D., Pawelski, H. & Reuter, S. Imaging-based diagnosis of acute renal allograft rejection. *World J Transplant.* Mar 24; **6**(1), 174–82 (2016).
- Hanssen, O. *et al.* Non-invasive approaches in the diagnosis of acute rejection in kidney transplant recipients. Part I. *In vivo* imaging methods. *Clin Kidney J. Feb*; **10**(1), 97–105 (2017).
- Ercicum, P. *et al.* Non-invasive approaches in the diagnosis of acute rejection in kidney transplant recipients, part II: omics analyses of urine and blood samples. *Clin Kidney J. Feb*; **10**(1), 106–115 (2017).
- Lovinfosse, P. *et al.* Fluorodeoxyglucose F(18) Positron Emission Tomography Coupled With Computed Tomography in Suspected Acute Renal Allograft Rejection. *Am. J. Transplant.* **16**, 310–316 (2016).
- Grabner, A. *et al.* PET with ^{18}F -FDG-labeled T lymphocytes for diagnosis of acute rat renal allograft rejection. *J Nucl Med.* Jul; **54**(7), 1147–53 (2013).
- Reuter, S. *et al.* Potential of noninvasive serial assessment of acute renal allograft rejection by ^{18}F -FDG PET to monitor treatment efficiency. *J. Nucl. Med.* **51**, 1644–1652 (2010).

19. Haas, M. *et al.* Banff 2013 meeting report: inclusion of c4d-negative antibody-mediated rejection and antibody-associated arterial lesions. *Am. J. Transplant.* **14**, 272–283 (2014).
20. Adams, M. C., Turkington, T. G., Wilson, J. M. & Wong, T. Z. A systematic review of the factors affecting accuracy of SUV measurements. *AJR.* **195**, 310–320 (2010).
21. Pawelski, H. *et al.* SPECT- and PET-based approaches for noninvasive diagnosis of acute renal allograft rejection. *Bio Med. Res. Int.* **2014**, 874785 (2014).
22. Grabner, A. *et al.* Non-invasive imaging of acute allograft rejection after rat renal transplantation using 18F-FDG PET. *J. Vis. Exp.* **74**(Apr 28), e4240 (2013).
23. Hanssen, O. *et al.* Diagnostic yield of 18 F-FDG PET/CT imaging and urinary CXCL9/creatinine levels in kidney allograft subclinical rejection. *Am J Transplant.* Dec 16 (2019).
24. Minamimoto, R., Takahashi, N. & Inoue, T. FDG-PET of patients with suspected renal failure: standardized uptake values in normal tissues. *Ann. Nucl. Med.* **21**, 217–222 (2007).
25. Jadoul, A. *et al.* The Uptake of 18F-FDG by Renal Allograft in Kidney Transplant Recipients Is Not Influenced by Renal Function. *Clin Nucl Med. Sep*; **41**(9), 683–7 (2016).
26. Akers, S. R., Werner, T. J., Rubello, D., Alavi, A. & Cheng, G. 18F-FDG uptake and clearance in patients with compromised renal function. *Nucl Med Commun.* Aug; **37**(8), 825–32 (2016).
27. Engel, H. *et al.* Whole-body PET: physiological and artifactual fluorodeoxyglucose accumulations. *J. Nucl. Med.* **37**, 441–446 (1996).
28. Benz, M. R. *et al.* Treatment monitoring by 18F-FDG PET/CT in patients with sarcomas: interobserver variability of quantitative parameters in treatment-induced changes in histopathologically responding and nonresponding tumors. *J Nucl Med.* Jul; **49**(7), 1038–46 (2008).
29. Huang, Y. E. *et al.* Interobserver variability among measurements of the maximum and mean standardized uptake values on (18) F-FDG PET/CT and measurements of tumor size on diagnostic CT in patients with pulmonary tumors. *Acta Radiol. Sep*; **51**(7), 782–8 (2010).
30. Büyükdere, G., Güler, M. & Şeydaoğlu, G. Interobserver and Intraobserver Variability among Measurements of FDG PET/CT Parameters in Pulmonary Tumors. *Balkan Med J. May*; **33**(3), 308–15 (2016).
31. Goh, V. *et al.* Integrated (18)F-FDG PET/CT and perfusion CT of primary colorectal cancer: effect of inter- and intraobserver agreement on metabolic-vascular parameters. *AJR Am J Roentgenol.* Nov; **199**(5), 1003–9 (2012).
32. Sorof, J. M. *et al.* Histopathological concordance of paired renal allograft biopsy cores. Effect on the diagnosis and management of acute rejection. *Transplantation.* Dec 15; **60**(11), 1215–9 (1995).
33. Jin, C., Shi, F., Xiang, D., Zhang, L. & Chen, X. Fast segmentation of kidney components using random forests and ferns. *Med Phys.* Dec; **44**(12), 6353–6363 (2017).
34. Lodge, M. A. Repeatability of SUV in Oncologic 18F-FDG PET. *J Nucl Med.* Apr; **58**(4), 523–532 (2017).
35. Paquet, N., Albert, A., Foidart, J. & Hustinx, R. Within-patient variability of (18)F-FDG: standardized uptake values in normal tissues. *J Nucl Med.* May; **45**(5), 784–8 (2004).

Author contributions

A.J. analyzed all PET/CT, interpreted the data and wrote the manuscript. P.L. analyzed all PET/CT and interpreted the data. L.W. was a major contributor in the enrollment of the population. A.B. and H.P. make the statistical analysis. R.H. and F.J. interpreted the data. The manuscript have been reviewed and approved by all authors.

Competing interests

The authors declare no competing interests.

Additional information

Supplementary information is available for this paper at <https://doi.org/10.1038/s41598-020-61032-z>.

Correspondence and requests for materials should be addressed to F.J.

Reprints and permissions information is available at www.nature.com/reprints.

Publisher's note Springer Nature remains neutral with regard to jurisdictional claims in published maps and institutional affiliations.



Open Access This article is licensed under a Creative Commons Attribution 4.0 International License, which permits use, sharing, adaptation, distribution and reproduction in any medium or format, as long as you give appropriate credit to the original author(s) and the source, provide a link to the Creative Commons license, and indicate if changes were made. The images or other third party material in this article are included in the article's Creative Commons license, unless indicated otherwise in a credit line to the material. If material is not included in the article's Creative Commons license and your intended use is not permitted by statutory regulation or exceeds the permitted use, you will need to obtain permission directly from the copyright holder. To view a copy of this license, visit <http://creativecommons.org/licenses/by/4.0/>.

© The Author(s) 2020